

OXYGEN-ENRICHED COMBUSTION MECHANISM OF LIGNITE

by

Xiangyun CHEN^a, Yongfeng ZHANG^{b*}, and Yinmin ZHANG^b

^a College of Textile and Light Industry, Inner Mongolia University of Technology, Hohhot, China

^b College of Chemical Engineering, Inner Mongolia University of Technology, Hohhot, China

Original scientific paper

<https://doi.org/10.2298/TSCI2004411C>

In this work, thermogravimetric experiments were carried out in a thermogravimetric analyzer under O₂/N₂ atmosphere with an oxygen content ranging from 21 vol.% to 70 vol.%. Malek method combined with iso-conversional method and non-isothermal method was employed to determine the burning dynamical function of lignite in high temperature burning region with different oxygen concentrations. The results indicated that the lignite has different burning dynamical function in different oxygen conditions. The combustion mechanism function of lignite belonged to 3-D model when the oxygen concentration is below 30%. The combustion mechanism of lignite belongs to a random successive nucleation growth model when the oxygen concentration is between 40% and 50%. Kinetic burning model of lignite in high burning temperature region with different oxygen concentrations was established. The kinetic parameters were obtained from the kinetic burning model of lignite using Kissinger-Akah-Sunose method.

Key words: oxygen-enriched, lignite, mechanism function, kinetics

Introduction

The lignite coal regions of Inner Mongolia account for 75% of the total lignite in China [1]. Most researchers have concluded that the coal combustion process is greatly affected by the O₂ concentration [2, 3].

Kinetics is always a good tool to exploring the mechanism of coal combustion, and thermal analysis is a recognized method to study coal combustion kinetics. Iso-conversional methods enable us to determine kinetic parameters without knowledge of reaction mechanism, and Kissinger-Akah-Sunose (KAS) model allows the calculation of the activation energy of the process, which uses dynamic integral and differential thermogravimetric (TG) curves to obtain several heating rates, parameters of thermal decomposition reaction, such as activation energy, E , pre-exponential factor, A , and the functional $f(\alpha)$ [4], which represents a relationship between the reaction rate and the conversion rate, that is the reaction mechanism. Different researchers got the kinetic parameters in the non-isothermal kinetic analysis with a single heat rate, one of the reasons is that the form of $f(\alpha)$ is different from the actual kinetic process. Therefore, it is very important to choose a logical form of $f(\alpha)$.

The purpose of this work is to investigate the most probably combustion mechanism function of the lignite in O₂/N₂ atmosphere with different oxygen concentrations by Malek method. The thermal analysis kinetics models were explored for lignite in high temperature region.

* Corresponding author, e-mail: lzg05006@163.com

Theory and data

Solid state kinetics of the decomposition reaction can be explained:

$$\frac{d\alpha}{dt} = k(T)f(\alpha) \quad (1)$$

The integration of eq. (1) gives directly:

$$G(\alpha) = \int_0^{\alpha} \frac{d\alpha}{f(\alpha)} = k(T)t \quad (2)$$

where α is the conversion extent, $\alpha = W_0 - W/W_0 - W_{\infty}$, W_0 and W_{∞} are sample masses at the beginning, and the end of mass loss reaction, respectively, W – the sample mass, $f(\alpha)$ – the differential form of the reaction model, $G(\alpha)$ – the integral form of the reaction model, T – the temperature, $k(T)$ – the reaction rate constant which is described by Arrhenius equation, $k(T) = A \exp(-E/RT)$, where A is the pre-exponential factor, E – the apparent activation energy, and R – the gas constant (8.314 J/molK). Equations (1) and (2) can be converted into eqs. (3) and (4), respectively:

$$\frac{d\alpha}{dT} = \left(\frac{A}{\beta}\right) \exp\left(-\frac{E}{RT}\right) f(\alpha) \quad (3)$$

$$\int_0^{\alpha} \frac{d\alpha}{f(\alpha)} = G(\alpha) = \frac{A}{\beta} \int_0^T \exp\left(-\frac{E}{RT}\right) dT \quad (4)$$

where $\beta = dT/dt$, it is a constant heating rate.

If E/RT is replaced by x , eq. (4) can be written:

$$G(\alpha) = \frac{AE}{\beta R} \int_x^{+\infty} \frac{\exp(-x)}{x^2} dx = \frac{AE}{\beta R} P(x) \quad (5)$$

where $P(x)$ in eq. (5) is the temperature integral and has no analytical form, but has many simplified approximations. The KAS is based on Newtonian approximation which is $P(x) = x^{-2}e^{-x}$.

Equation (5) can be transformed into:

$$\ln\left(\frac{\beta}{T^2}\right) = \ln\left[\frac{AE}{RG(\alpha)}\right] - \frac{E}{RT} \quad (6)$$

The E for different conversion values can be calculated from a plotting $\ln(\beta/T^2)$ vs. $1/T$.

Malek method was used to infer mechanism function $f(\alpha)$ or $G(\alpha)$. Combining eqs. (3) and (4), we can get:

$$G(\alpha) = \frac{RT^2}{E\beta} \frac{d\alpha}{dt} \frac{1}{f(\alpha)} \quad (7)$$

When $\alpha = 0.5$, it becomes:

$$G(0.5) = \frac{RT_{0.5}^2}{E\beta} \left(\frac{d\alpha}{dt} \right)_{0.5} \frac{1}{f(0.5)} \quad (8)$$

Dividing eq. (7) by eq. (8), eq. (9) is obtained:

$$y(\alpha) = \frac{f(\alpha)G(\alpha)}{f(0.5)G(0.5)} \quad (9-1)$$

$$y(\alpha) = \frac{T}{T_{0.5}} \frac{\frac{d\alpha}{dt}}{\left(\frac{d\alpha}{dt} \right)_{0.5}} \quad (9-2)$$

On the basis of eq. (9-1), the plots of $y(\alpha)$ vs. α of different mechanism function models can be obtained. Taking the thermogravimetric experiment data into eq. (9-2), experimental plots of $y(\alpha)$ vs. α can be obtained. If the experimental plots match with the model plots well, the mechanism function will be the most probable mechanism function of the reaction. In the paper, 15 kinetics mechanism functions shown in tab. 1 were selected to verify which one best fits the reduction reaction.

Table 1. Differential and integral expression of the kinetics mechanism functions

Symbol	Reaction	$G(\alpha)$	$f(\alpha)$
1	Parabola rule (1-D diffusion)	α^2	$-(1/2)\alpha^{-1}$
2	Valensi (2-D diffusion)	$\alpha + (1 - \alpha)\ln(1 - \alpha)$	$[-\ln(1 - \alpha)]^{-1}$
3	G-B (3-D diffusion)	$1 - 2/3 \alpha - (1 - \alpha)2/3$	$(3/2)[(1 - \alpha)^{-1/3} - 1]$
4	Z-L-T (3-D diffusion)	$[(1 - \alpha)^{-1/3} - 1]$	$(3/2)(1 - \alpha)^{4/3}[(1 - \alpha)^{-1/3} - 1]$
5	Mamplé (A1, F1, $n = 1, m = 1$)	$-\ln(1 - \alpha)$	$1 - \alpha$
6	A-E ($n = 3/2$)	$[-\ln(1 - \alpha)]^{3/2}$	$2/3(1 - \alpha)[- \ln(1 - \alpha)]^{-1/2}$
7	A-E ($n = 2$)	$[-\ln(1 - \alpha)]^2$	$1/2(1 - \alpha)[- \ln(1 - \alpha)]^{-1}$
8	A-E ($n = 3$)	$[-\ln(1 - \alpha)]^3$	$1/3(1 - \alpha)[- \ln(1 - \alpha)]^{-2}$
9	A-E ($n = 4$)	$[-\ln(1 - \alpha)]^4$	$1/4(1 - \alpha)[- \ln(1 - \alpha)]^{-3}$
10	Tertiary chemical reaction (F3)	$(1 - \alpha)^{-2}$	$1/2(1 - \alpha)^3$
11	Secondary chemical reaction (F2)	$(1 - \alpha)^{-1}$	$(1 - \alpha)^2$
12	Shrink cylinder (R2)	$1 - (1 - \alpha)^{1/2}$	$2(1 - \alpha)^{1/2}$
13	Contraction sphere ($n = 1/3$)	$1 - (1 - \alpha)^{1/3}$	$3(1 - \alpha)^{2/3}$
14	3-D ($n = 3$)	$3[1 - (1 - \alpha)^{1/3}]$	$(1 - \alpha)^{2/3}$
15	Jander (D3, 3-D)	$[1 - (1 - \alpha)^{1/3}]$	$3/2(1 - \alpha)^{2/3}[1 - (1 - \alpha)^{1/3}]^{-1}$

The value of E can also be obtained by Coats-Redfern method, which is fit for non-isothermal method with single heating rate, considering Frank-Kamenetskii approximation which is $P(x) = e^{-x/x^2}$ in eq. (5), we get the Coats-Redfern Integral type as given in:

$$\ln \frac{G(\alpha)}{T^2} = \ln \frac{AR}{\beta E} - \frac{E}{RT} \quad (10)$$

Activation energy can be calculated from plotting $\ln[G(\alpha)]/T^2$ with $1/T$.

Experimental

Iso-conversional methods thermal experiments were performed using a Netzsch STA 409PC analyzer with a steady air flow of 80 mL per minute. Approximately 10 mg YBS lignite less than 80 μm was heated from room temperature to 1273 K at three different heating rates (5, 10, 25 K per minute). The tests were conducted in an O_2/N_2 atmosphere with the O_2 concentration is 21, 40, 70 vol.%, respectively.

Non-isothermal thermal experiments were conducted in O_2/N_2 atmosphere with the O_2 concentrations of 21, 30, 40, 50, 60, and 70 vol.%, respectively, the heating rate is 10 K per minute.

Results and discussion

The KAS method

The TG curves and the characteristic temperature in different oxygen concentrations and heating rates had been offered in our previous researches [5, 6].

According to KAS method in eq. (6), by plotting the linear relationship of $\ln(\beta/T^2)$ against $1/T$, activation energy, E , of the lignite in different oxygen concentrations can be estimated at various conversions α ranging from 0.2 to 0.8, which is shown in fig. 1 and tab. 2.

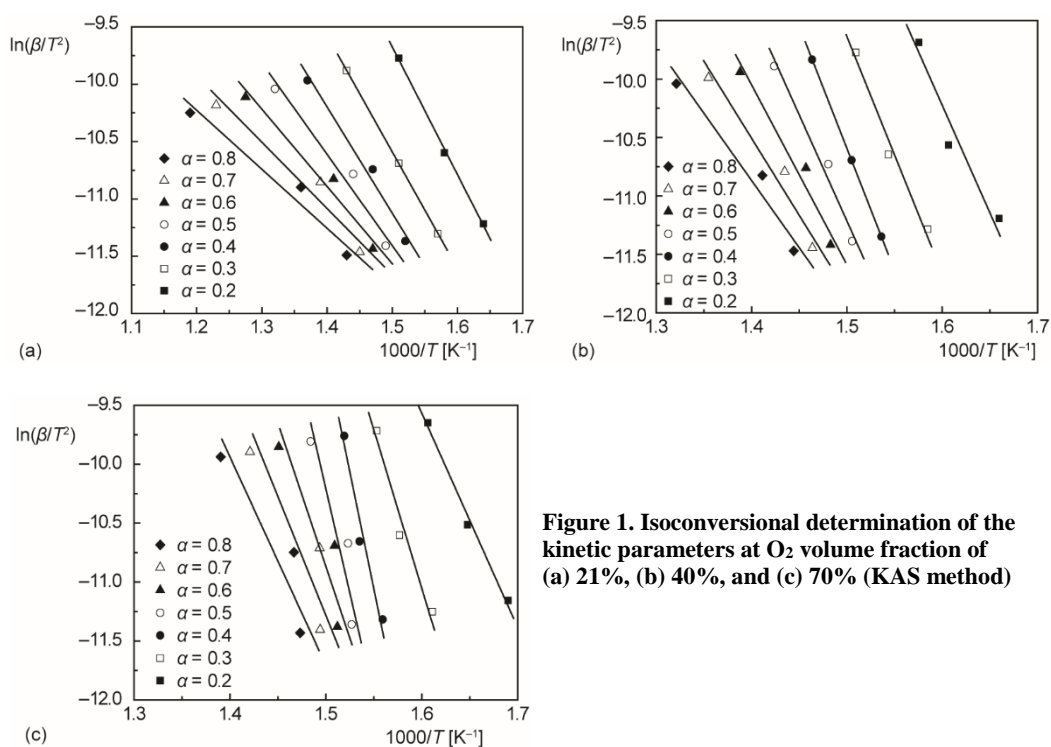


Figure 1. Isoconversional determination of the kinetic parameters at O_2 volume fraction of (a) 21%, (b) 40%, and (c) 70% (KAS method)

Malek method

The $y(\alpha) - \alpha$ curves were used to infer the most probable mechanism function [7, 8]. Putting the data gotten from each mechanism function of tab. 1 to eq. (9-1), and putting the experiment data to eq. (9-2), we obtain the result as showed in fig. 2.

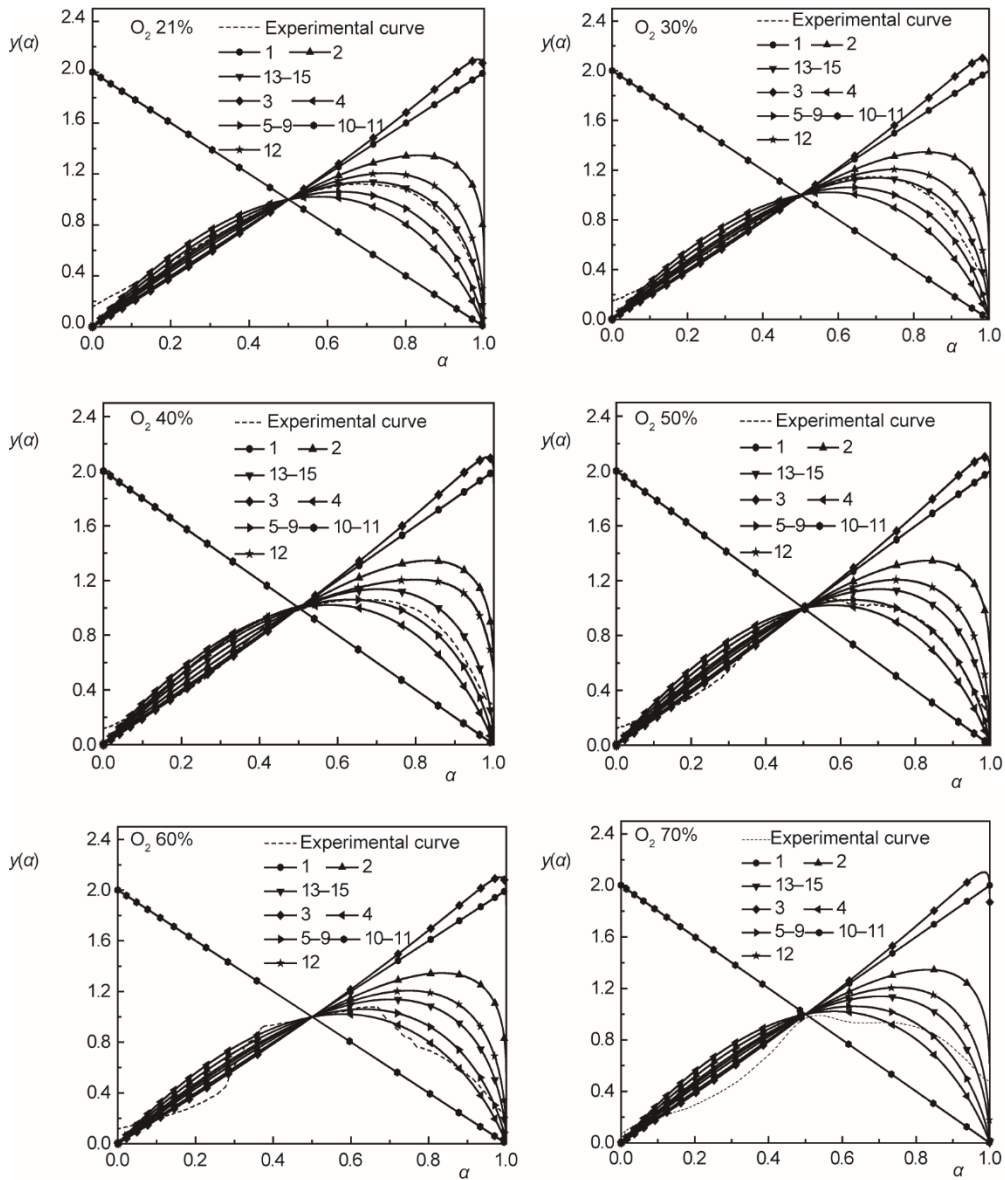


Figure 2. The $y(\alpha) - \alpha$ curve in different oxygen concentration

Figure 2 showed that the curve was divided into high temperature and low temperature according to point $\alpha = 0.5$. We studied the mechanism function of high temperature. It

can be seen from fig. 2, experimental plots match with No. 13-15 models well when the oxygen concentration is below 30%, so No. 13-15 in tab. 1 are the probable mechanism function of the reaction. Experimental plots match with No. 5-9 models well when the oxygen concentration is between 40-50%. The mechanism function cannot be confirmed when the oxygen concentration is above 60% because of the intensity and complexity response.

Table 2. The activation energies obtained by TG data at different rates by KAS methods

α	O ₂ :N ₂ = 21:79		O ₂ :N ₂ = 40:60		O ₂ :N ₂ = 70:30	
	E [kJmol ⁻¹]	R	E [kJmol ⁻¹]	R	E [kJmol ⁻¹]	R
0.2	92.52	-0.99927	143.82	-0.96977	149.84	-0.99554
0.3	84.45	-0.99999	164.84	-0.98964	215.09	-0.98102
0.4	75.80	-0.99172	173.51	-1.0000	315.49	-0.97874
0.5	64.03	-0.98314	147.37	-0.98856	253.66	-0.92897
0.6	54.38	-0.98512	123.13	-0.98130	167.60	-0.91040
0.7	45.61	-0.97407	105.03	-0.97909	133.06	-0.91119
0.8	40.93	-0.97806	91.55	-0.97865	123.95	-0.91853
Average	65.39		135.61		194.10	

In order to determine the most probably mechanism function, the activation energy was obtained by Coats-Redfern method in eq. (10) according to the aforementioned probable mechanism functions. The results were shown in tab. 3.

Table 3. The values of E according to different mechanism function

O ₂ :N ₂ = 21:79	Mechanism function No.	E [kJmol ⁻¹]
21:79	13	71.50
	14	71.50
	15	131.84
40:60	5	123.88
	6	191.66
	7	259.50
	8	395.16
	9	530.82

Compared between tabs. 2 and 3, the similar values of E are the most probable mechanism functions. The No. 13 and 14 are the most probably mechanism functions when the oxygen concentration is below 30%. The No. 5 is the most probably mechanism function when the oxygen concentration is between 40-50%.

To verify the mechanism function, we consider $f(\alpha)$ in eq. (3), and obtain:

$$\frac{d\alpha}{dT} = \left(\frac{A}{\beta}\right) \exp\left(-\frac{E}{RT}\right) (1-\alpha)^{2/3} \quad (11)$$

$$\frac{d\alpha}{dT} = 3 \left(\frac{A}{\beta} \right) \exp \left(-\frac{E}{RT} \right) (1-\alpha)^{2/3} \quad (12)$$

$$\frac{d\alpha}{dT} = \left(\frac{A}{\beta} \right) \exp \left(-\frac{E}{RT} \right) (1-\alpha) \quad (13)$$

The calculated curves and the experimental curves of $d\alpha/dT$ vs. T were shown in fig. 3. Equations (11)-(13) can be effectively solved by the variational iteration method [9], the homotopy perturbation method [10-12] and Taylor method [13], for the engineering problem, a simple analytical method is much welcome for practical applications [14, 15].

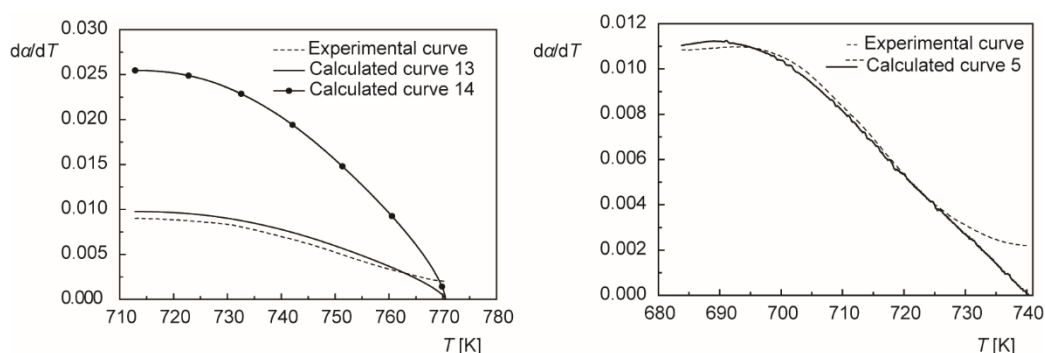


Figure 3. Experimental and calculated curve in different oxygen concentration

It can be seen from fig. 3 that the calculated curve of Nos. 13 and 5 were in a good agreement with the experimental results, so the most probably mechanism functions were confirmed.

Conclusion

This paper combined the results of iso-conversional TG analysis and non-isothermal TG analysis with single heat rate. The most probably combustion mechanism functions of lignite in different oxygen concentrations were got by Malek method in high burning temperature region. The combustion mechanism of lignite belongs to a 3-D model when the oxygen concentration is below 30%. However, the combustion mechanism function belongs to random successive nucleation growth model with the oxygen concentration ranging from 40% to 50%. It is difficult to confirm the mechanism function in the high oxygen concentration such as above 60%.

Acknowledgment

The work is supported by National Natural Science Foundation of China (21066009), Inner Mongolia Natural Science Foundation (2017MS(LH)0206).

References

- [1] Yin, L. Q., Lignite Resources and Utilization Outlook in China, (in Chinese), *Coal Science and Technology*, 32 (2004), 2, pp. 12-14
- [2] Zhou, Z. J. et al., Oxy-Fuel Combustion Characteristics and Kinetic Parameters of Lignite Coal from thermo-gravimetric Data, *Thermochimica Acta*, 553 (2013), 2, pp. 54-59

- [3] Daood, S. S., et al., Deep-Staged, Oxygen Enriched Combustion of Coal, *Fuel*, 101 (2012), Nov., pp. 187-196
- [4] Arisoy, A., et al., Reaction Kinetics of Coal Oxidation at Low Temperatures, *Fuel*, 159 (2015), Nov., pp. 412-417
- [5] Chen, X. Y., et al., Thermal Analyses of the Lignite Combustion in Oxygen-Enriched Atmosphere, *Thermal Science*, 19 (2015), 3, pp. 801-811
- [6] Zhang, Y. F., et al., Oxygen-Enriched Combustion of Lignite, *Thermal Science*, 19 (2015), 4, pp. 1389-1392
- [7] Tang, Y. T., et al., Oxidation Mechanism and Non-isothermal Kinetic Studies on Carbonate iron ore by Thermogravimetric Analysis, *Journal of Iron and Steel Research International*, 25 (2018), 12, pp. 1223-1231
- [8] Huo, L. M., et al., Oxidation and Reduction Kinetic of $\text{YBaCo}_4\text{O}_{7+\delta}$ and Substituted Oxygen Carriers, *Journal of Thermal Analysis and Calorimetry*, 134 (2018), 3, pp. 2213-2221
- [9] Anjum, N., He, J. H., Laplace Transform: Making the Variational Iteration Method Easier, *Applied Mathematics Letters*, 92 (2019), June, pp. 134-138
- [10] He, J. H., Some Asymptotic Methods for Strongly Nonlinear Equations, *International Journal of Modern Physics B*, 20 (2006), 10, pp. 1141-1199
- [11] Ren, Z. F., et al., He's Multiple Scales Method for Nonlinear Vibrations, *Journal of Low Frequency Noise, Vibration and Active Control*, 38 (2019), 3-4, pp. 1708-1712
- [12] Yu, D. N., et al., Homotopy Perturbation Method with an Auxiliary Parameter for Nonlinear Oscillators, *Journal of Low Frequency Noise, Vibration and Active Control*, 38 (2019), 3-4, pp. 1540-1554
- [13] He, J. H., Ji, F. Y., Taylor Series Solution for Lane-Emden Equation, *Journal of Mathematical Chemistry*, 57 (2019), 8, pp. 1932-1934
- [14] He, J. H., The Simplest Approach to Nonlinear Oscillators, *Results in Physics*, 15 (2019), 102546
- [15] He, J. H., The Simpler, the Better: Analytical Methods for Nonlinear Oscillators and Fractional Oscillators, *Journal of Low Frequency Noise, Vibration and Active Control*, 38 (2019), 3-4, pp. 1252-1260